Bacterial adhesion onto nanofiltration and reverse osmosis membranes: Effect of permeate flux

Bacterial adhesion onto nanofiltration and reverse osmosis membranes: effect of permeate flux

Andrea J.C. Semião[1], Olivier Habimana[2], Eoin Casey[2]*

[1]School of Engineering, University of Edinburgh, UK EH9 3JL

[2]School of Chemical and Bioprocess Engineering, University College Dublin (UCD) , IRELAND

*Corresponding author. Mailing address: University College Dublin, School of Chemical and Bioprocess Engineering, Belfield, Dublin 4, IRELAND. Phone: +353 1 716 1877, Email: eoin.casey@ucd.ie

KEYWORDS: bacterial adhesion, permeate flux, nanofiltration, reverse osmosis, biofouling

Abstract

The influence of permeate flux on bacterial adhesion to NF and RO membranes was examined using two model *Pseudomonas* species, namely *Pseudomonas fluorescens* and *Pseudomonas putida*. To better understand the initial biofouling profile during NF/RO processes, deposition experiments were conducted in cross flow under permeate flux varying from 0.5 up to 120 L/(h.m^2), using six NF and RO membranes each having different surface properties. All experiments were performed at a Reynolds number of 579. Complementary adhesion experiments were performed using *Pseudomonas* cells grown to early-, mid- and late-exponential growth phases to evaluate the effect of bacterial cell surface properties during cell adhesion under permeate flux conditions. Results from this study show that initial bacterial adhesion is strongly dependent on the permeate flux conditions, where increased adhesion was obtained with increased permeate flux, until a maximum of 40% coverage was reached. Membrane surface properties or bacterial growth stages was further found to have little impact on bacterial adhesion to NF and RO membrane surfaces under the conditions tested. These results emphasise the importance of conducting adhesion and biofouling experiments under realistic permeate flux conditions, and raises questions about the efficacy of the methods for the evaluation of antifouling membranes in which bacterial adhesion is commonly assessed under zero-flux or low flux conditions, unrepresentative of full-scale NF/RO processes.

41 # 1. Introduction
42
43 Nanofiltration (NF) and Reverse Osmosis (RO) are well-established processes for the
44 production of high quality water. NF is principally used for the removal of hardness, trace
45 contaminants, such as pesticides and organic matter (Cyna et al. 2002), while RO is used for
46 desalination (Greenlee et al. 2009). NF and RO performance are however adversely affected by
47 biofilm formation resulting in permeate flux and quality decline (Flemming 1997, Ivnitsky et al. 2007,
48 Houari et al. 2009, Vrouwenvelder et al. 1998, Vrouwenvelder et al. 2008, Khan et al. 2013),
49 generally caused by the initial adhesion and subsequent colonization of bacterial cells on the surface
50 of the membrane, amalgamating in a biomass consisting of, and not limited to, polysaccharides,
51 proteins, and extracellular DNA (Pamp et al. 2007).

52 The first stage of biofilm formation is initiated by the adhesion of bacteria to the membrane
53 surface, a precursor of biofilm formation (Costerton et al. 1995). Previous studies have shown that
54 NF and RO membrane properties (Lee et al. 2010, Myint et al. 2010, Bernstein et al. 2011), bacterial
55 properties (Bayoudh et al. 2006, Bakker et al. 2004, Mukherjee et al. 2012) and environmental
56 conditions affect bacterial adhesion (Sadr Ghayeni et al. 1998). However, most of these studies were
57 conducted without permeate flux, which is an inherent part of NF and RO processes. The
58 hydrodynamic and concentration polarisation effects associated with flux may alter the micro-
59 environmental conditions at the interface thereby playing an important role in the characteristics
60 and rate of bacterial adhesion. A recent study showed that under the same flux conditions, the
61 biofilm formed on the surface of three different RO membranes had similar characteristics and
62 affected the membrane performance to the same extent (Baek et al. 2011): the percentage flux
63 decline was identical for all the membranes studied. In a previous study (Suwarno et al. 2012) it was
64 shown that higher permeate flux resulted in increased biovolume on the membrane surface.
65 Although previous studies suggest biofilm formation is independent of membrane surface properties

66 but dependent on pressure, no systematic studies to date have attempted to investigate the
67 relationship between initial adhesion and membrane properties at different flux conditions.

68 Surprisingly, few studies have focused on bacterial deposition under permeate flux
69 conditions (Kang et al. 2006, Kang et al. 2004, Subramani and Hoek 2008, Subramani et al. 2009,
70 Eshed et al. 2008). These studies focussed on developing an understanding of the fundamental
71 mechanisms of bacterial attachment under permeate flux conditions, often combined with the DLVO
72 theory (Derjaguin-Landau-Verwey-Overbeek theory), which describes the interactions between a
73 bacterial cell and the membrane surface taking into account Lifshitz–van der Waals (LW) and
74 electrostatic double layer (EL) interactions combined with interfacial hydrodynamic forces of cross-
75 flow lift (CL), permeation drag (PD), and gravity (G). The XDLVO theory (Extended Derjaguin-Landau-
76 Verwey-Overbeek theory) also takes into account Lewis acid–base (AB) interactions between the
77 bacterial cell and the membrane surface. Cross-flow lift (CL), permeation drag (PD), and gravity (G)
78 forces dominate bacterial movement. If the drag due to the permeating liquid is strong enough to
79 counteract the lifting force associated with cross-flow, the bacteria will be drawn towards the
80 membrane surface where it will be subjected to short range forces such as Lifshitz-van der Waal's,
81 electrostatic double layer (EL) and Lewis acid-base interactions (AB).

82 The only studies where bacterial deposition specifically to NF and RO membranes under
83 permeate flux conditions were reported, are those from Subramani *et al.* (Subramani and Hoek
84 2008, Subramani et al. 2009) where it was found that bacterial adhesion was influenced by
85 membrane properties. However, these studies were conducted at comparatively low fluxes, of less
86 than 20 L/(h.m^2) (equivalent to 2.5 bar). In full-scale NF and RO processes for water, seawater and
87 brackish water, treatment fluxes can reach up to 70 L/(h.m^2) (Cyna et al. 2002, Greenlee et al. 2009,
88 Houari et al. 2009, Ventresque et al. 2000). One of the conclusions of the previous study (Subramani
89 and Hoek 2008) was that adhesion increases with permeate flux and according to the XDLVO theory,
90 permeation drag overwhelms interfacial forces at fluxes greater than 20 L/(h.m^2) for Reynolds

numbers Re<200. Furthermore, the study also concluded that the higher the Reynolds number, the lower the level of concentration polarisation will be encountered for NF and RO membranes, translating into increased electrostatic double layer repulsion between the negatively charged bacteria and the negatively charged membrane, hence reducing adhesion rates. A high cross-flow velocity is also expected to decrease adhesion due to enhanced cross-flow lift. In fact Wang et al. (Wang et al. 2005) showed that increasing cross-flow velocity after adhesion experiments could cause adhered bacteria to detach: this was particularly effective for adhesion permeate fluxes below a "critical flux" whereby DLVO repulsion was in excess of permeation drag and bacteria adhered reversibly.

A higher Reynolds number combined with a higher permeate flux have therefore opposing effects, and it is unclear how adhesion would be influenced by permeate fluxes and Reynolds numbers used in full scale NF and RO applications. To our knowledge, there are no reports in the literature concerning bacterial adhesion at fluxes greater than 20 L/(h.m^2) for NF/RO membranes or at Reynolds numbers representative of spiral wound elements in full-scale plants where values range between 150 and 2000 (Schock and Miquel 1987).

For the broader range of membrane processes, conflicting results can be found in the literature. One study showed adhesion rates onto MF membranes subjected to permeate fluxes ~70 L/(h.m^2) to be considerably different between membranes with different surface properties (Kang et al. 2006). In contrast, another study (Subramani and Hoek 2008) observed a decrease in the differences of adhesion rates as one increased the permeate flux through several NF and RO membranes from no permeate flux up to ~20 L/(h.m^2). A clear gap in the knowledge of bacterial adhesion to NF and RO membranes was therefore identified, where the mechanisms of adhesion under common cross-flow and pressure filtration conditions for different commercially available NF and RO membranes needed to be clarified.

This paper therefore investigates the initial adhesion of two bacterial strains, *Pseudomonas fluorescens* and *Pseudomonas putida,* to 6 different NF and RO membranes under industrially relevant permeate flux conditions, as well as the adhesion of *P. fluorescens* at different growth stages. *Pseudomonas*, including *Pseudomonas fluorescent* and *putida* are commonly found in NF and RO biofilms during water treatment (Ivnitsky et al. 2007, Sadr Ghayeni et al. 1998, Baker and Dudley 1998).

2. Materials and Methods

2.1 Model Bacteria Strains and Media

The selected model bacterial strains for this study were fluorescent mCherry-expressing *Pseudomonas fluorescens* PCL1701 (Lagendijk et al. 2010) and *Pseudomonas putida* PCL1480 (Lagendijk et al. 2010). *Pseudomonas* strains were stored at -80°C in King B broth (King et al. 1954) supplemented with 20% glycerol. Cultures of both *Pseudomonas fluorescens* and *Pseudomonas putida* were obtained by inoculating 100 mL King B broth supplemented with gentamicin at a final concentration of 10 $\mu g.mL^{-1}$ using respective single colonies previously grown on King B agar (Sigma Aldrich, Ireland) at 28°C. Subsequently, cultures were incubated at 28°C with shaking at 75 rpm and left to grow to early exponential, mid exponential or late exponential growth stages, corresponding to Optical Densities (OD_{600}) of 0.2, 0.6 and 1.0, respectively, for the study of the impact of bacteria growth stage on adhesion to NF and RO membranes. The experiments for the study of the impact of flux on the adhesion of bacteria *P. fluorescens* and *P. putida* to different NF and RO membranes were performed using cells in their late exponential growth stage (OD_{600}=1.0).

2.2 Microbial Adhesion to Solvents

Microbial adhesion to solvents (MATS) (BellonFontaine et al. 1996) was used as a method to determine the hydrophobic and Lewis acid–base surface properties of *P. fluorescens* cells at different growth stages. This method is based on the comparison between microbial cell surface affinity to a monopolar solvent and an apolar solvent, which both exhibit similar Lifshitz-van der Waals surface tension components. Hexadecane (nonpolar solvent), chloroform (an electron acceptor solvent), decane (nonpolar solvent) and ethyl acetate (an electron donor solvent) were used of the highest purity grade (Sigma-Aldrich, USA). Experimentally, overnight bacterial cultures grown at different stages (early, mid and late exponential phase) were washed twice in sterile 0.1 M NaCl solution as described in section 2.3, and re-suspended to a final OD_{400} of 0.8. Individual bacterial suspensions (2.4 ml) were vortexed for 60 seconds with 0.4 ml of their respective MATS solvent. The mixture was allowed to stand for 15 min to ensure complete separation of phases. One mL from the aqueous phase was then removed using glass Pasteur pipettes and the final OD_{400} was measured. The percentage of cells residing in the solvent was calculated by the following equation:

$$\%\text{Adherence} = \frac{(\text{OD}_\text{i} - \text{OD}_\text{f})}{\text{OD}_\text{i}} \times 100$$

where (OD_i) is the initial optical density of the bacterial suspension before mixing with the solvent, and (OD_f) the final absorbance after mixing and phase separation. Each measurement was performed in triplicate.

2.3 Cell preparation for adhesion assay

To evaluate bacterial adhesion under different flux conditions, cell concentration for each growth stage (i.e. early exponential, mid exponential or late exponential growth stages) was standardized by diluting the growth cultures to a final OD_{600} of 0.2 in 200 mL 0.1 M NaCl (Sigma-Aldrich, Ireland). This ensured a standardized starting feed cell concentration before every adhesion assay, in which

controlled experiments with different parameters (i.e. permeate flux and growth stage) could be compared and studied. For cells grown to early exponential phase two 100 mL cultures were prepared.

Cells were then harvested by centrifugation at 5000 rpm for 10 min using a Sorval RC5C Plus centrifuge (Unitech, Ireland) and a FiberliteTM f10-6x500y fixed angle rotor (Thermo Fisher Scientific Inc., Dublin, Ireland). The supernatant was carefully discarded and the pellet re-suspended in 200 mL 0.1 M NaCl solution, resulting in an inoculum consisting of approximately 10^8 cells/mL. This process was performed twice. A solution of 0.1 M NaCl was used as a model solution to mimic brackish water characteristics (Greenlee et al. 2009).

2.4 Membranes and Cross-flow Test Unit

Six NF and RO membranes were used: NF90, NF270, BW30 and BW30 FR (Dow Filmtec Corp, USA) and ESNA1-LF and ESNA1-LF2 from Hydranautics (Nitto Denko Corp, USA). BW30 FR stands for Fouling Resistant membrane. The membrane properties are presented in Table 1

Table 1 Membrane Properties

	Permeability (L/(h.m^2.bar))[a]	NaCl Retention[b] (%)	Contact Angle[c] (°)	Roughness R_{MS}[d] (nm)
NF90	6.8±0.5	87.8±4.0	58.4±0.6	484.0 ± 207.1
NF270	12.6±1.2	16.0±0.3	8.4±0.5	372.9 ± 246.4
BW30	2.6±0.3	93.5±2.1	25.6±0.8	209.0 ± 41.9
BW30 FR	2.8±0.5	92.9±1.3	62.2±0.6	665.7 ± 156.9
ESNA1- LF	3.5±0.4	88.8±1.5	68.8±0.6	214.5 ± 23.4
ESNA1 – LF2	6.8±0.8	75.2±0.2	62.4±0.7	661.3 ± 97.7

[a] Permeability measured with MilliQ water at 21°C
[b] 0.1 M NaCl at 15 bar, 21ºC and Re=579

[c] Mean contact angle of a total of 20 deionized water droplets on two independent membrane samples using a goniometer (OCA 20 from Dataphysics Instruments)
[d] 45 µm ×59 µm of area measured using a Wyko NT1100 optical profilometer operating in vertical scanning interferometry (VSI) mode

As can be seen from Table 1 membrane surface properties varied substantially, with contact angles, membrane surface roughness, and salt retention parameters ranging from 8.5° to 68.8°, 214.5 up to 665.7 nm and 16.0 to 93.5%, respectively. These results clearly show the variability in surface hydrophobicity as well as topographic profile of the selected membranes.

The cross-flow test unit used was a modified version of the unit found in a previous study (Semião et al. 2013) and the schematic and operational details can be found in the Supporting Information SI. Three Membrane Fouling Simulator (MFS) devices of internal channel dimensions of 0.8 mm in height, 40 mm width and 255 mm length were used in parallel. No feed spacers were used in this study.

2.5 Cleaning Protocol

The protocol used to clean the cross-flow system consisted of two antibacterial treatments involving 30 min recirculation steps of 70% Industrial Methylated Spirit (IMS, Lennox, Dublin, Ireland), followed by 0.1 M NaOH. The system was rinsed in between treatments with 18.2 $m\Omega.cm^{-1}$ grade 1 pure water (Elgastat B124, Veolia, Ireland). Since pure water is ineffective in completely removing NaOH, an added step of recirculating pure water with a pH adjusted to 7 using 5 M HCl and a buffer solution of 10 mM $NaHCO_3$ was adopted. The pH of the recirculating solution was systematically checked to ensure there was no vestige of NaOH in the system. The system was then thoroughly rinsed with pure water. No adhesion of fluorescent cells on a membrane compacted for 18 hours with pure water occurred, showing the efficiency of the washing method.

207

208

209 **2.6 Adhesion Protocol**

210 Three different membranes were cut, thoroughly rinsed with pure water and left soaking overnight
211 in the fridge at 4°C. The membranes were then inserted in the cross-flow system and compacted for
212 a minimum of 18 hours at 21°C with pure water. The membrane pure water flux was measured at 15
213 bar and at the pressure subsequently used during the adhesion experiment. The cross-flow system
214 was operated in total recirculation mode (i.e. recirculation of the retentate and permeate), ensuring
215 the feed concentration and volume during the experimental runs were constant.

216 A 4 L volume of 0.1 M NaCl solution was then inserted in each feed tank (tank 1 and tank 2) and
217 recirculated in the system to remove any air bubbles. Then feed tank 2 was blocked with the ball
218 valve system and only feed tank 1 was used. Prior to inserting the bacterial cells in feed tank 1, the
219 cross-flow system was left to equilibrate at a constant selected pressure and cross-flow of 0.66
220 $L.min^{-1}$ (Re=579 or cross flow velocity of 0.35 $m.s^{-1}$) for 15 minutes with the 0.1 M NaCl solution in
221 tank 1. Selected experimental conditions consisted of monitoring bacterial adhesion at pressures
222 ranging from 3.1 to 15.5 bar, with corresponding membrane fluxes ranging up to 70 $L/(h.m^2)$ at a
223 constant temperature of 21°C. This range of fluxes was chosen to ensure coverage of the range used
224 in typical full-scale applications of NF and RO processes (Cyna et al. 2002, Greenlee et al. 2009,
225 Houari et al. 2009, Ventresque et al. 2000). In the specific case of the NF 270 membrane this range
226 was extended to 120 $L/(h.m^2)$ purely for scientific reasons, for example in the case where novel
227 membranes can operate at higher fluxes than the ones commonly applied in today's water
228 treatment plants. A bacterial inoculum containing approximately 10^8 cells/mL was then added to
229 feed tank 1 and recirculated in the system for 30 minutes at the constant filtration conditions of
230 pressure and cross-flow as the ones used during equilibration. Permeate flux, feed and permeate

conductivity were measured for each membrane cell before (i.e. during equilibration with 0.1 M NaCl) and after bacterial inoculation (i.e. during bacterial adhesion). After 30 minutes of adhesion, feed tank 2 outlet with 0.1 M NaCl solution was opened and feed tank 1 outlet was closed in order to rinse any non-adhered bacterial cells from the system under the filtration conditions used prior to *ex-situ* analysis of the bacterial adhesion. Every experiment was repeated at least twice. The effect of rinsing and the effect of opening the MFS for *ex-situ* analysis of bacterial surface coverage was investigated by comparison with a control study performed with an MFS fitted with a sapphire glass window for *in-situ* measurements. The results of these control studies are described in the Supplemental Information (S2).

2.7 Adhesion quantification

Membrane Fouling Simulator (MFS) cells were separated from the system at the end of adhesion experiments, and carefully opened whilst submerged in 0.1 M NaCl solution. The fouled membranes were removed, 3 pieces cut from different locations of the membrane and each sample was placed at the bottom of small petri dishes submerged with 0.1 M NaCl solution. The submerged fouled membranes were then observed under an epi-fluorescence microscope (Olympus BX51) using a 10X objective. Fluorescent mCherry-tagged *Pseudomon*as cells were observed using a 550 nm filter cube. Ten micrographs were obtained at random points from each membrane sample. Cell surface coverage (%) was then determined for each membrane using ImageJ® software, a Java-based image processing program (http://rsbweb.nih.gov/ij/). The emission intensity of the mCherry tagged *Pseudomonas cells* was found to be perfectly distinguishable from the autofluorescent background of the tested membranes. In some instances, the mCherry to background fluorescence signal was further improved by controlling the level of excitation light through samples using fluorescence excitation balancers, attached in parallel to the light path, and by adjusting the field iris diaphragm (Supporting information: S4). Acquired images were subsequently grayscaled and thresholded.

Bacterial deposition on membranes was then estimated as the percentage of solid surface covered by bacteria, based on the number of black and white pixels of thresholded images.

3. Results and Discussion

3.1 Effect of flux on *Pseudomonas fluorescens* adhesion

The effect of permeate flux on the initial adhesion of *P. fluorescens* for different NF and RO membranes is presented in Figure 1. The surface coverage of all 6 membranes was found to increase from 1.6±0.2% for a permeate flux of 0.5±0.1 L/(h.m^2) (0.14 µm.s^{-1}) for the BW30 FR up to 39.4±3.3% for a permeate flux of 35.47±0.01 L/(h.m^2) (9.9 µm.s^{-1}) for the ESNA 1-LF2. The range of permeate fluxes was extended for the particular case of the NF270 membrane, as stated in the Materials and Methods section. It was found that an increase of the permeate flux from 35.47 L/(h.m^2) to 116 L/(h.m^2) did not significantly increase the surface coverage which was constant at around 40%. Similarly, a previous study involving yeast on microfiltration membranes also correlated increased cell deposition with increased permeate flux (Kang et al. 2004). Nonetheless, this present study shows that bacterial adhesion reached a maximum surface coverage of around 40% for permeate fluxes higher than 36 L/(h.m^2) as shown for membranes NF270 and ESNA1-LF2. Ridgway et al. (Ridgway et al. 1984) also observed a similar plateau of adhered bacteria to a RO membrane. The authors hypothesized the adhesion plateau effect to be the direct result of a limiting number of adhesion sites available, independent of the increased bacterial concentration during the course of the fouling experiment. More recent studies, however, have demonstrated a blocking effect caused by the presence of previously adhered particles, colloids or bacterial cells (Sjollema and Busscher 1990, Ko and Elimelech 2000, Busscher and van der Mei 2006, Kerchove and Elimelech 2008): particles or bacteria already adhered on the membrane surface can hinder bacterial adhesion on the membrane surface in nearby areas causing adhesion to eventually reach a maximum.

280 Differences between a “nearly linear” adhesion (Kang et al. 2004) with increased permeate flux and
281 an adhesion that reaches a plateau, as observed in this study, could also be explained by the
282 differences in cell feed concentration. As shown in an earlier study (Kang et al. 2004), differences in
283 cell feed concentration led to significant differences in the amount of bacteria adhered when
284 subjected to identical filtration conditions; the degree of membrane fouling on a membrane will be
285 directly proportional to the bacterial concentration used, where the lower the bacterial
286 concentration, the lower the number of adhered bacterial cells.

287 NF and RO membranes have been shown to vary substantially in their surface properties. For
288 example, surface contact angle have been previously reported to range between 38.6º and 73.2º,
289 the root mean square (RMS) roughness to range between 5.9 and 130 nm and the zeta potential
290 measurement to range between -4.0 and -19.7 mV for several commercial NF and RO membranes
291 (Norberg et al. 2007). Moreover, previous studies investigating bacterial adhesion onto NF and RO
292 membranes clearly demonstrate the role of membrane surface properties on bacterial adhesion, in
293 which attributes such as membrane hydrophobicity, surface charge and roughness have shown to
294 significantly influence bacterial adhesion (Lee et al. 2010, Myint et al. 2010, Bernstein et al. 2011,
295 Kang et al. 2006, Subramani and Hoek 2008). The quantitative differences in adhesion between the
296 studied membranes were large, with bacteria adhering to some membranes up to 21 times more
297 than others. However, as previously mentioned, these studies were carried out under the absence of
298 or under very low pressure conditions (<2.5 bar), and/or at very low Reynolds numbers (Re<80). One
299 of the objectives of this study was to investigate bacterial adhesion using realistic hydrodynamic
300 conditions in order to mimic NF and RO spiral-wound modules. It was observed that NF and RO
301 membrane surface properties had a small effect on bacterial adhesion under the wide range of
302 permeate flux conditions tested. The highest significant differences were obtained in the region of
303 permeate fluxes of 20 L/(h.m^2), where surface coverage varied from 17.1±2.8% for the NF270 with a
304 flux of 19.0±1.3 L/(h.m^2) up to 32.5±0.7% for the ESNA1-LF with a flux of 18.8±0.1 L/(h.m^2). This
305 translates to the ESNA1-LF adhering only 1.8 times more than the NF270, which comparatively to the

previous mentioned studies (Lee et al. 2010, Suwarno et al. 2012, Kang et al. 2004) is a small difference. The small differences obtained in surface coverage for these two membranes is probably due to the fact that the NF270 membrane is more hydrophilic with a contact angle of 8.4° compared to the ESNA1-LF which has a more hydrophobic nature, with a contact angle of 68.8°, as can be seen in Table 1. Hence the more hydrophobic membrane ESNA1-LF shows greater adhesion compared to the more hydrophilic membrane NF270.

When comparing the other membranes for a permeate flux in the region of 20 L/(h.m^2), it can be seen from Figure 1 that surface coverage does not vary substantially: BW30 FR with a flux of 21.2±5.3 L/(h.m^2) has a surface coverage of 27.6±5.9%, the BW30 with a flux of 21.3±0.3 L/(h.m^2) has a surface coverage of 28.5±1.3% and the ESNA1-LF2 with a flux of 18.1±3.5 L/(h.m^2) has a surface coverage of 29.6±0.2%. The properties of the membranes tested are however very different, as can be seen in Table 1: the contact angle measurements varied from 25.6° for the BW30 to 62.4° for the ESNA1-LF2 and the roughness varied from 209 nm for the BW30 to 665.7 nm for the BW30-FR. Despite the significant differences of the membrane surface properties surface coverage did not vary substantially for the same permeate flux conditions, showing that under pressure membrane surface properties have a small effect on *P. fluorescens* adhesion (Figure S3.1 in the Supporting Information). This suggests that membranes with anti-bacterial or anti-biofouling properties should be tested under representative pressures in order to fully assess their true performance. In contrast, adhesion rates onto microfiltration membranes subjected to a permeate flux similar to the ones tested in the present paper (20 µm.s^{-1}) were considerably different depending on the membrane surface properties (Kang et al. 2006). These differences might be due to the tested species characteristics, to different filtration conditions, different membrane surface properties such as the presence of pores or to solution characteristics.

It was further noticed that the 30 min adhesion of bacterial cells to the membrane surface did not cause a decrease in the measured permeate flux as this did not vary by more than 3% compared to

331 the flux measured before the introduction of bacterial cells into the system (i.e. during equilibration
332 with 0.1 M NaCl). Despite the adhesion of bacterial cells to the membrane surface covering up to
333 40% of the surface, this did not cause enhanced concentration polarisation that has been identified
334 in previous studies in the case of cake and biofilm formation (Herzberg and Elimelech 2007, Hoek
335 and Elimelech 2003).

336 Two main conclusions can be drawn from this study at the experimental conditions studied: (1) *P.*
337 *fluorescens* adhesion is dependent on the permeate flux and does not substantially vary for different
338 membrane properties; (2) *P. fluorescens* adhesion reached a maximum of surface coverage of 40%
339 for permeate flux higher than 35.5 L/(m^2.h^1).

340

341 **3.2 Effect of flux on *Pseudomonas putida* adhesion**

342 *P. putida* was employed as an alternative species in a similar series of experiments to those
343 conducted with *P. fluorescens*. The results shown in Figure 2 can be seen to follow the same trend
344 as observed with *P. fluorescens* with surface coverage increasing with permeate flux. It is clear that
345 the membrane surface properties do not have a substantial impact on the rate of bacterial adhesion
346 for the conditions tested. For a flux of 13.8±0.9 L/(h.m^2) NF90 has a surface coverage of 15.5±0.9%,
347 the BW30 FR with a flux of 19.6±1.7 L/(h.m^2) has a surface coverage of 16.9±3.0% and the NF270
348 with a flux of 19.0±0.3 L/(h.m^2) has a surface coverage of 15.0 ±1.2%. The properties of the surfaces
349 of the membranes tested are however very different with respect to contact angle and roughness, as
350 can be seen in Table 1, showing that as for *P. fluorescens*, membrane surface properties have an
351 insubstantial effect on *P. putida* adhesion under permeate flux conditions (Figure S3.2 in the
352 Supporting Information).

353 The only difference noticed between the two bacterial species tested, *P. fluorescens* and *P. putida*,
354 was in the surface coverage rate as a function of the permeate flux (Figure 2): *P. fluorescens* reaches
355 a maximum coverage of about 40% at a permeate flux between 40 and 60 L/(h.m^2) whilst *P. putida*

356 reaches a surface coverage of 40% for permeate fluxes higher than 100 L/(h.m^2). These differences
357 could be associated to small differences of bacteria size. The smaller bacteria *P. putida* suffers
358 permeate drag to a lesser extent than *P. fluorescens* (Subramani and Hoek 2008) and therefore
359 adheres less for similar permeate fluxes. However due to the previously described "blocking effect"
360 mechanism, surface saturation is eventually reached by both strains at ~40% surface coverage. As *P.*
361 *fluorescens* and *P. putida* do not substantially differ in cell size, the blocking effect caused by these
362 two strains would be expected to be similar, and therefore the maximum surface coverage reached
363 is also expected to be similar.

364 The study by Subramani and Hoek (Subramani and Hoek 2008) showed that during filtration at low
365 pressures, the difference in adhesion rates between species studied was significant, but as the
366 pressure increased, corresponding to fluxes up to 20 L/(h.m^2), the difference in adhesion rates
367 between species diminished resulting in similar adhesion rates at higher pressures/permeate fluxes
368 regardless of species studied. Furthermore, the same study (Subramani and Hoek 2008) showed
369 that the differences in adhesion rate of *Saccharomyces cerevisiae* on different tested membranes
370 became smaller with increasing permeate flux conditions, hence showing an overwhelming effect of
371 the convective flux compared to membrane surface properties. Although this present study differs
372 from the previous studies by focusing primarily on "end-points" following 30 minutes adhesion, a
373 common conclusion can be drawn in which higher permeate flux will lead to higher bacterial surface
374 coverage but membrane and cell surface properties have very little impact on the surface coverage.
375 The design of this present study therefore allowed a comparison of multiple membranes at different
376 flux conditions in regards to bacterial adhesion, which was especially necessary when evaluating the
377 claimed anti-fouling properties of specialized commercial membranes.
378
379
380

3.3 Effect of bacterial growth stage deposition under flux conditions

During bacterial adhesion the outer cell membrane is usually the first point of contact when interacting with abiotic surfaces. The bacterial outer membrane functions as a permeability barrier regulating the passage of solutes between the cell and the surrounding environment, determining the physicochemical properties of the cell (Caroff and Karibian 2003, Makin and Beveridge 1996, Gargiulo et al. 2007). Surface macromolecules such as lipopolysacchides and surface proteins that constitute the outer membrane have been shown to significantly influence the physicochemical properties of bacterial cells (van Loosdrecht et al. 1987). Moreover, the composition of macromolecules on the outer membrane is known to be influenced by the bacterial growth phase (Hong and Brown 2006). In one recent study (Walker et al. 2005) it was shown that the adhesion profile of *Escherichia coli* was dependent on its growth phase, which was determined by the charge distribution resulting from electrostatic repulsion forces. Differences in biofouling of RO membranes have also been shown to depend on the growth stage of the bacterial species studied (Herzberg et al. 2009). Differences were caused by the bacterial cell properties such as zeta potential. It is however unclear how the growth stage impacts on the initial adhesion of bacteria onto NF and RO membranes at high flux conditions. Hence the initial biofouling onto different NF and RO membranes was investigated in the present study at a fixed but representative pressure (11.3 bar) using bacteria at different growth phases to determine whether the effect of cell surface physico-chemistry was significant. The physicochemical surface properties of *P. fluorescens* cells grown at different exponential growth stages based on their affinities to different polar and apolar solvents were studied and are presented in Table 2. Considerable variations in the affinity of *P. fluorescens* cells to apolar solvents hexadecane and decane revealed changes in surface hydrophobicities as cells enter into different exponential growth stages. Affinity to hexadecane decreased from 67.2 % to 27.0%, as cells enter early exponential (OD_{600}=0.2) to late exponential (OD_{600}=1.0) growth stages. Likewise affinities to decane decreased from 47.6% to 28.9%.

A high affinity to chloroform (>94%) was observed for all tested *P. fluorescens* cells, irrespective of their growth stage. The high affinity to chloroform compared to affinities to hexadecane is an indication that the tested *P. fluorescens* cells possess a dominating electron donor character. Although lower, the affinities to ethyl acetate were on average ≈50%, irrespective of *P. fluorescens* growth state. When comparing affinities to decane and ethyl acetate, *P. fluorescens* cells grown to mid exponential (OD_{600}=0.6) and to late exponential phases (OD_{600}=1.0) possess a secondary electron acceptor character, based on their higher affinity to ethyl acetate than decane. This Lewis acid surface property is negligible for *P. fluorescens* cells entering early exponential growth stage (OD_{600}=0.2) as seen by their similar affinities to both decane and ethyl acetate. These results clearly indicate the subtle surface physicochemical differences between *P. fluorescens* grown at different exponential stages. Surface hydrophobicity has been shown to affect cell adhesion to surfaces (Bos et al. 1999, Habimana et al. 2007, Vanloosdrecht et al. 1987).

Table 2: Mean affinities of *P. fluorescens* at different growth stages to solvents hexadecane, chloroform, decane, and ethyl acetate. Error represents standard deviation of three replicates.

Growth stage OD_{600}	Solvents			
	Hexadecane	Chloroform	Decane	Ethyl Acetate
0.2	67.2 ± 0.6	96.0 ± 0.2	47.6 ± 0.5	44.6 ± 5.0
0.6	41.4 ± 7.4	94.4 ± 0.9	24.1 ± 2.3	53.7 ± 3.3
1	27.0± 1.1	94.4 ± 1.2	28.9± 0.8	52.8 ± 1.1

In the particular case of *P. fluorescens*, there is no significant effect of the growth stage on the adhesion onto different NF and RO membranes, as shown in Figure 3 (and Figure S3.2 in the Supporting Information). It seems that the convective flux towards the membrane surface overcomes the effect of the membrane surface properties, as suggested in a previous study (Subramani and Hoek 2008).

4. CONCLUSION

This study offers an increased understanding of bacterial adhesion on NF/RO membranes under conditions typically found in full-scale processes. The work presented in this paper clearly shows that for representative Reynolds numbers and permeate fluxes, the membrane properties and bacterial growth phases do not substantially affect initial bacterial adhesion. This has very important implications, particularly for studies where anti-biofouling membranes are under evaluation: the true efficiency of these membranes can only be fully evaluated when tested under realistic permeate flux conditions. Future work will also need to examine biological factors involved during the early stage of membrane fouling such as EPS synthesis. An understanding of these factors would help better devise or select optimal processing strategies for controlling the level of fouling during NF/RO processes. Furthermore, membranes labelled as Fouling Resistant such as the BW30 FR have been shown to have the same initial bacterial adhesion outcome as the other membranes when subjected to typical flux conditions of NF and RO membranes: the surface modifications carried out on this membrane were not sufficient to avoid bacterial adhesion. This poses an important question: will an efficient anti-biofouling membrane ever be developed? Should future research focus on anti-adhesion surfaces or should it focus on more efficient cleaning strategies?

Acknowledgments

This research was supported by the European Research Council (ERC), project 278530, funded under the EU Framework Programme 7. The authors would like to thank Mr. Pat O'Halloran for his invaluable technical assistance, and Mr. Liam Morris for the construction of the MFS devices. The authors especially thank Dr. Ellen L. Lagendijk from the Institute of Biology Leiden, Netherlands for the gift of the *Pseudomonas fluorescens* WCS365, PCL1701 and *Pseudomonas putida* PCL 1445, PCL

455 1480 strains. The authors would final like to thank Hydranautics for kindly providing samples of the
456 ESNA1-LF and ESNA1-LF 2 membranes.

457

458 **References**

459 Cyna, B., Chagneau, G., Bablon, G. and Tanghe, N. (2002) Two years of nanofiltration at the Méry-
460 sur-Oise plant, France. Desalination 147(1–3), 69-75.

461 Greenlee, L.F., Lawler, D.F., Freeman, B.D., Marrot, B. and Moulin, P. (2009) Reverse osmosis
462 desalination: Water sources, technology, and today's challenges. Water Research 43(9), 2317-2348.

463 Flemming, H.C. (1997) Reverse osmosis membrane biofouling. Experimental Thermal and Fluid
464 Science 14(4), 382-391.

465 Ivnitsky, H., Katz, I., Minz, D., Volvovic, G., Shimoni, E., Kesselman, E., Semiat, R. and Dosoretz, C.G.
466 (2007) Bacterial community composition and structure of biofilms developing on nanofiltration
467 membranes applied to wastewater treatment. Water Research 41(17), 3924-3935.

468 Houari, A., Seyer, D., Couquard, F., Kecili, K., Démocrate, C., Heim, V. and Martino, P.D. (2009)
469 Characterization of the biofouling and cleaning efficiency of nanofiltration membranes. Biofouling
470 26(1), 15-21.

471 Vrouwenvelder, H.S., van Paassen, J.A.M., Folmer, H.C., Hofman, J.A.M.H., Nederlof, M.M. and van
472 der Kooij, D. (1998) Biofouling of membranes for drinking water production. Desalination 118(1–3),
473 157-166.

474 Vrouwenvelder, J.S., Manolarakis, S.A., van der Hoek, J.P., van Paassen, J.A.M., van der Meer, W.G.J.,
475 van Agtmaal, J.M.C., Prummel, H.D.M., Kruithof, J.C. and van Loosdrecht, M.C.M. (2008) Quantitative
476 biofouling diagnosis in full scale nanofiltration and reverse osmosis installations. Water Research
477 42(19), 4856-4868.

478 Khan, M.T., Manes, C.-L.d.O., Aubry, C. and Croué, J.-P. (2013) Source water quality shaping different
479 fouling scenarios in a full-scale desalination plant at the Red Sea. Water Research 47(2), 558-568.

480 Pamp, S.J., Gjermansen, M. and Tolker-Nielsen, T. (2007) The biofilm matrix: a sticky framework,
481 Horizon BioScience, Wymondham, UK.

482 Costerton, J.W., Lewandowski, Z., Caldwell, D.E., Korber, D.R. and Lappin-Scott, H.M. (1995)
483 Microbial biofilms. Annual Reviews in Microbiology 49(1), 711-745.

484 Lee, W., Ahn, C.H., Hong, S., Kim, S., Lee, S., Baek, Y. and Yoon, J. (2010) Evaluation of surface
485 properties of reverse osmosis membranes on the initial biofouling stages under no filtration
486 condition. Journal of Membrane Science 351(1–2), 112-122.

487 Myint, A.A., Lee, W., Mun, S., Ahn, C.H., Lee, S. and Yoon, J. (2010) Influence of membrane surface
488 properties on the behavior of initial bacterial adhesion and biofilm development onto nanofiltration
489 membranes. Biofouling 26(3), 313-321.

490 Bernstein, R., Belfer, S. and Freger, V. (2011) Bacterial Attachment to RO Membranes Surface-
491 Modified by Concentration-Polarization-Enhanced Graft Polymerization. Environmental Science &
492 Technology 45(14), 5973-5980.

493 Bayoudh, S., Othmane, A., Bettaieb, F., Bakhrouf, A., Ouada, H.B. and Ponsonnet, L. (2006)
494 Quantification of the adhesion free energy between bacteria and hydrophobic and hydrophilic
495 substrata. Materials Science and Engineering: C 26(2–3), 300-305.

496 Bakker, D.P., Postmus, B.R., Busscher, H.J. and van der Mei, H.C. (2004) Bacterial Strains Isolated
497 from Different Niches Can Exhibit Different Patterns of Adhesion to Substrata. Applied and
498 Environmental Microbiology 70(6), 3758-3760.

499 Mukherjee, J., Karunakaran, E. and Biggs, C.A. (2012) Using a multi-faceted approach to determine
500 the changes in bacterial cell surface properties influenced by a biofilm lifestyle. Biofouling 28(1), 1-
501 14.

502 Sadr Ghayeni, S.B., Beatson, P.J., Schneider, R.P. and Fane, A.G. (1998) Adhesion of waste water
503 bacteria to reverse osmosis membranes. Journal of Membrane Science 138(1), 29-42.

504 Baek, Y., Yu, J., Kim, S.-H., Lee, S. and Yoon, J. (2011) Effect of surface properties of reverse osmosis
505 membranes on biofouling occurrence under filtration conditions. Journal of Membrane Science
506 382(1–2), 91-99.

507 Suwarno, S.R., Chen, X., Chong, T.H., Puspitasari, V.L., McDougald, D., Cohen, Y., Rice, S.A. and Fane,
508 A.G. (2012) The impact of flux and spacers on biofilm development on reverse osmosis membranes.
509 Journal of Membrane Science 405–406(0), 219-232.

510 Kang, S., Hoek, E.M.V., Choi, H. and Shin, H. (2006) Effect of Membrane Surface Properties During
511 the Fast Evaluation of Cell Attachment. Separation Science and Technology 41(7), 1475-1487.

512 Kang, S.-T., Subramani, A., Hoek, E.M.V., Deshusses, M.A. and Matsumoto, M.R. (2004) Direct
513 observation of biofouling in cross-flow microfiltration: mechanisms of deposition and release.
514 Journal of Membrane Science 244(1–2), 151-165.

515 Subramani, A. and Hoek, E.M.V. (2008) Direct observation of initial microbial deposition onto reverse
516 osmosis and nanofiltration membranes. Journal of Membrane Science 319(1–2), 111-125.

517 Subramani, A., Huang, X. and Hoek, E.M.V. (2009) Direct observation of bacterial deposition onto
518 clean and organic-fouled polyamide membranes. Journal of Colloid and Interface Science 336(1), 13-
519 20.

520 Eshed, L., Yaron, S. and Dosoretz, C.G. (2008) Effect of Permeate Drag Force on the Development of
521 a Biofouling Layer in a Pressure-Driven Membrane Separation System. Applied and Environmental
522 Microbiology 74(23), 7338-7347.

Ventresque, C., Gisclon, V., Bablon, G. and Chagneau, G. (2000) An outstanding feat of modern technology: the Mery-sur-Oise nanofiltration Treatment plant (340,000 m3/d). Desalination 131(1–3), 1-16.

Wang, S., Guillen, G. and Hoek, E.M.V. (2005) Direct Observation of Microbial Adhesion to Membranes†. Environmental Science & Technology 39(17), 6461-6469.

Schock, G. and Miquel, A. (1987) Mass transfer and pressure loss in spiral wound modules. Desalination 64, 339-352.

Baker, J.S. and Dudley, L.Y. (1998) Biofouling in membrane systems — A review. Desalination 118(1–3), 81-89.

Lagendijk, E.L., Validov, S., Lamers, G.E.M., de Weert, S. and Bloemberg, G.V. (2010) Genetic tools for tagging Gram-negative bacteria with mCherry for visualization in vitro and in natural habitats, biofilm and pathogenicity studies. Fems Microbiology Letters 305(1), 81-90.

King, E.O., Ward, M.K. and Raney, D.E. (1954) Two Simple Media for the Demonstration of Pyocyanin and Fluorescin. Journal of Laboratory and Clinical Medicine 44(2), 301-307.

BellonFontaine, M.N., Rault, J. and vanOss, C.J. (1996) Microbial adhesion to solvents: A novel method to determine the electron-donor/electron-acceptor or Lewis acid-base properties of microbial cells. Colloids and Surfaces B-Biointerfaces 7(1-2), 47-53.

Semião, A.J.C., Habimana, O., Cao, H., Heffernan, R., Safari, A. and Casey, E. (2013) The importance of laboratory water quality for studying initial bacterial adhesion during NF filtration processes. Water Research 47(8), 2909-2920.

Ridgway, H.F., Rigby, M.G. and Argo, D.G. (1984) Adhesion of a Mycobacterium sp. to cellulose diacetate membranes used in reverse osmosis. Applied and Environmental Microbiology 47(1), 61-67.

Sjollema, J. and Busscher, H.J. (1990) Deposition of polystyrene particles in a parallel plate flow cell. 2. Pair distribution functions between deposited particles. Colloids and Surfaces 47(0), 337-352.

Ko, C.-H. and Elimelech, M. (2000) The “Shadow Effect” in Colloid Transport and Deposition Dynamics in Granular Porous Media: Measurements and Mechanisms. Environmental Science & Technology 34(17), 3681-3689.

Busscher, H.J. and van der Mei, H.C. (2006) Microbial adhesion in flow displacement systems. Clinical microbiology reviews 19(1), 127-141.

Kerchove, A.J.d. and Elimelech, M. (2008) Bacterial Swimming Motility Enhances Cell Deposition and Surface Coverage. Environmental Science & Technology 42(12), 4371-4377.

555 Norberg, D., Hong, S., Taylor, J. and Zhao, Y. (2007) Surface characterization and performance
556 evaluation of commercial fouling resistant low-pressure RO membranes. Desalination 202(1–3), 45-
557 52.

558 Herzberg, M. and Elimelech, M. (2007) Biofouling of reverse osmosis membranes: Role of biofilm-
559 enhanced osmotic pressure. Journal of Membrane Science 295(1–2), 11-20.

560 Hoek, E.M.V. and Elimelech, M. (2003) Cake-Enhanced Concentration Polarization: A New Fouling
561 Mechanism for Salt-Rejecting Membranes. Environmental Science & Technology 37(24), 5581-5588.

562 Caroff, M. and Karibian, D. (2003) Structure of bacterial lipopolysaccharides. Carbohydrate Research
563 338(23), 2431-2447.

564 Makin, S.A. and Beveridge, T.J. (1996) The influence of A-band and B-band lipopolysaccharide on the
565 surface characteristics and adhesion of Pseudomonas aeruginosa to surfaces. Microbiology-Uk 142,
566 299-307.

567 Gargiulo, G., Bradford, S., Simunek, J., Ustohal, P., Vereecken, H. and Klumpp, E. (2007) Bacteria
568 transport and deposition under unsaturated conditions: The role of the matrix grain size and the
569 bacteria surface protein. Journal of Contaminant Hydrology 92(3-4), 255-273.

570 van Loosdrecht, M.C., Lyklema, J., Norde, W., Schraa, G. and Zehnder, A.J. (1987) The role of
571 bacterial cell wall hydrophobicity in adhesion. Appl Environ Microbiol 53(8), 1893-1897.

572 Hong, Y. and Brown, D.G. (2006) Cell surface acid-base properties of Escherichia coli and Bacillus
573 brevis and variation as a function of growth phase, nitrogen source and C : N ratio. Colloids and
574 Surfaces B-Biointerfaces 50(2), 112-119.

575 Walker, S.L., Hill, J.E., Redman, J.A. and Elimelech, M. (2005) Influence of growth phase on adhesion
576 kinetics of Escherichia coli D21g. Applied and Environmental Microbiology 71(6), 3093-3099.

577 Herzberg, M., Rezene, T.Z., Ziemba, C., Gillor, O. and Mathee, K. (2009) Impact of Higher Alginate
578 Expression on Deposition of Pseudomonas aeruginosa in Radial Stagnation Point Flow and Reverse
579 Osmosis Systems. Environmental Science & Technology 43(19), 7376-7383.

580 Bos, R., van der Mei, H.C. and Busscher, H.J. (1999) Physico-chemistry of initial microbial adhesive
581 interactions - its mechanisms and methods for study. Fems Microbiology Reviews 23(2), 179-230.

582 Habimana, O., Le Goff, C., Juillard, V., Bellon-Fontaine, M.N., Buist, G., Kulakauskas, S. and Briandet,
583 R. (2007) Positive role of cell wall anchored proteinase PrtP in adhesion of lactococci. Bmc
584 Microbiology 7.

585 Vanloosdrecht, M.C.M., Lyklema, J., Norde, W., Schraa, G. and Zehnder, A.J.B. (1987) Electrophoretic
586 Mobility and Hydrophobicity as a Measure to Predict the Initial Steps of Bacterial Adhesion. Applied
587 and Environmental Microbiology 53(8), 1898-1901.

588

List of figures

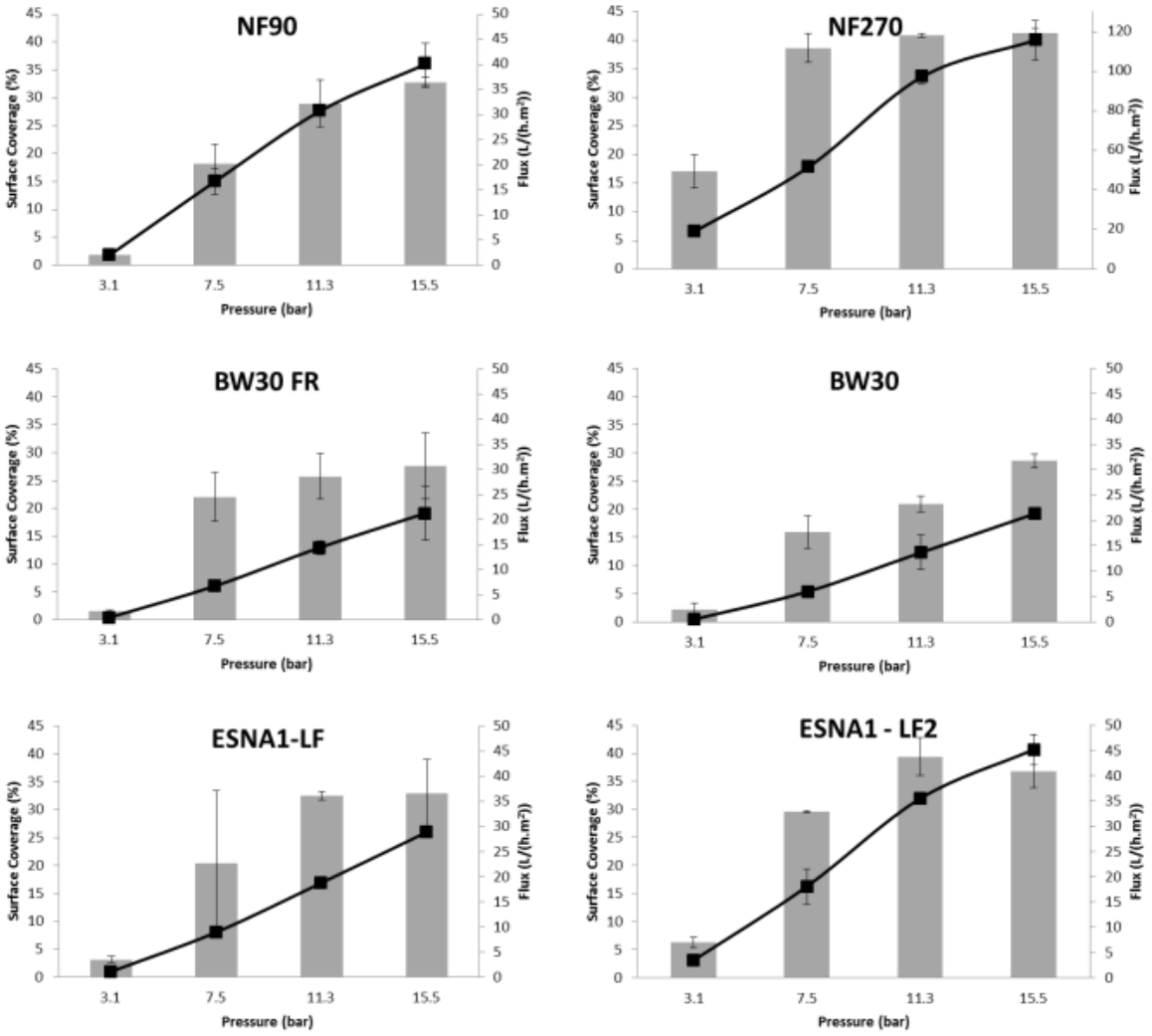

Figure 1: Effect of flux on *P. fluorescens* surface coverage of NF and RO membranes: columns represent surface coverage and black squares represent permeate flux (10^7 cells/mL, 0.1 M NaCl, 21°C, pH~7, 0.66 $L.min^{-1}$ or Re=579, each experiment repeated at least twice). Error bars show standard deviation of repeated experiments.

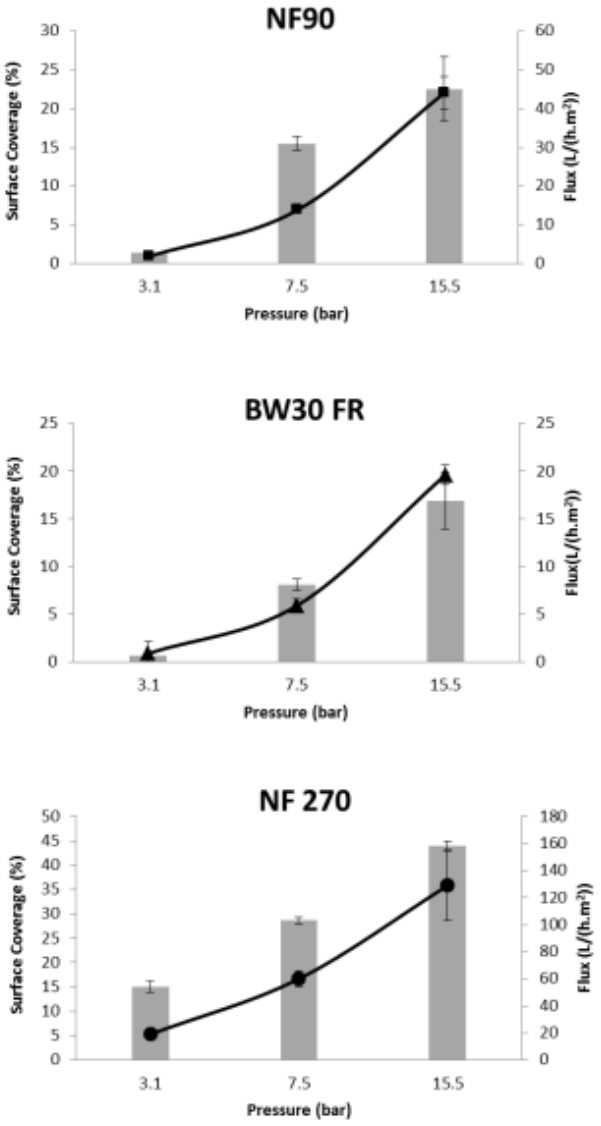

596

597 Figure 2: Effect of flux on *P. putida* surface coverage of NF and RO membranes: columns represent
598 surface coverage and black squares represent permeate flux (10^7 cells/mL, 0.1 M NaCl, 21°C, pH~7,
599 0.66 $L.min^{-1}$ or Re=579, each experiment repeated at least twice). Error bars show standard
600 deviation of repeated experiments. (Note: the permeate flux is apparently not seen as a linear
601 relationship with pressure because the columns are not equally spaced in pressure. The linear
602 correlation coefficient of permeate flux vs pressure is in fact r^2>0.995 for these experiments).

603

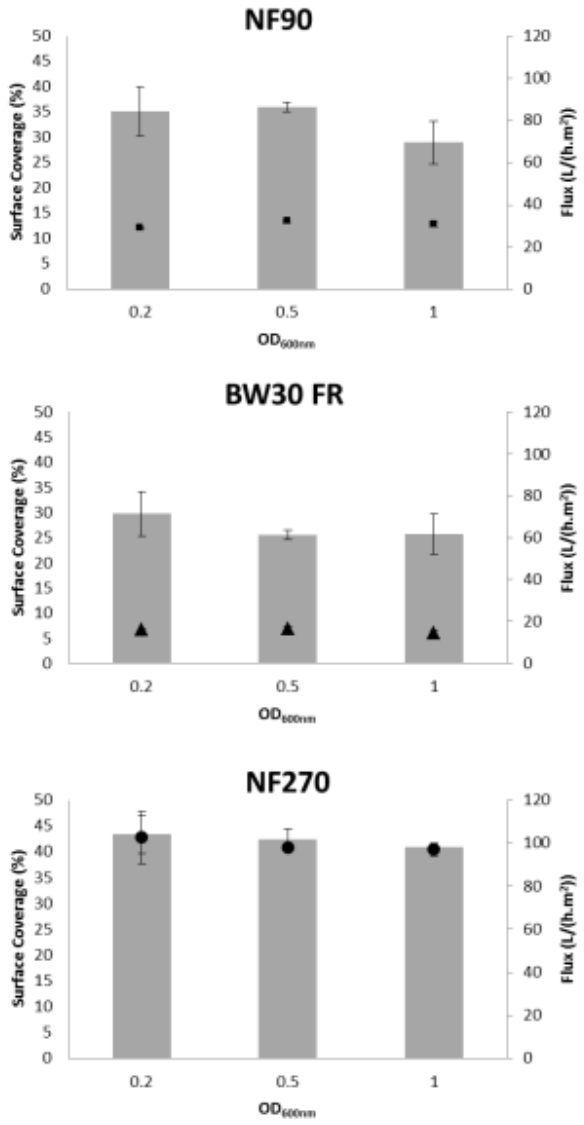

Figure 3: Effect of *P. fluorescens* growth stage on surface coverage of NF and RO membranes: columns represent surface coverage and black squares represent permeate flux (10^7 cells/mL, 0.1 M NaCl, 21°C, pH~7, 0.66 $L.min^{-1}$ or Re=579, 11.3 bar, each experiment repeated at least twice). Error bars show standard deviation of repeated experiments.